

Numerical research on the airflow distribution in mine tunnels

Cui DING^{a,*}, Xueqiu HE^{b,c}, Baisheng NIE^c

^aDepartment of Safety Engineering, China Institute of Industrial Relations, Beijing, China, 100048

^bSchool of Civil and Environment Engineering, University of Science and Technology Beijing, Beijing, China, 100083

^cSchool of Resource & Safety Engineering, China University Mining & Technology (Beijing), Beijing, China, 100083

ABSTRACT

Based on 3D modelling of typical tunnels in mines, the air flow structure in the three hearts arch-section tunnel was investigated and the influence of air velocity and cross section on air flow distribution in tunnels was studied. The average velocity points were analyzed quantitatively. The results showed that the feature of the air flow is similar with the shape of the three hearts arch-section under different ventilation velocities and cross section areas. The shape of the tunnel cross section and wall were the critical factors influencing the air flow structure. The average velocity points were mainly close to the tunnel wall. Characteristic equations were developed to describe the average velocity distribution, and provide the theoretical basis for accurately measuring the average velocity in mine tunnels.

KEYWORDS: mine tunnel; turbulence; air flow structure; three hearts arch; average velocity

1. INTRODUCTION

Mine ventilation is the process of continually inputting fresh air and outputting polluted air. The ventilation system is the basic system in mines. It is estimated that many mine disasters, including fire, coal gas, and dust explosions occur as a result of failures of the mine ventilation system.

Nowadays, the air flow velocity and volume in tunnels are detected by on-line monitoring systems. However, because of the non-uniform distribution of air flow, the velocity measured by sensors is not the average velocity in each section. As such, it is necessary to study the air flow structure, especially the average velocity distribution, so as to calculate the air flow volume accurately. At present, the air flow distribution in cross-sections is macroscopically described with numerical simulation in several studies (Parra et al., 2006; Chen and Yu, 2008; Jia, 2011; Hao et al., 2011). Only a few have quantitatively studied the average velocity distribution in circular and rectangular tunnels, by experimental and theoretical methods (Ma et al., 2007; Yin et al., 2008; Zhou et al., 2012; Wang et al., 2013; Tan et al., 2013; Zhao et al., 2014). However, the relations among the air flow structure, the average velocity, and the cross-section shape and sizes have not been developed and described successfully. The characteristic equations of the average velocity distribution close to the roof have been developed in the three hearts arch-section tunnels and trapezoidal cross section tunnels (Ding et al., 2015; Ding, 2016). The other areas of the average velocity distribution on three hearts arch-sections were not developed

quantitatively. This study aims to present the air flow distribution and develop the characteristic equations of the average velocity distribution in three hearts arch-section tunnels.

2. NUMERICAL SIMULATION

2.1 The physical model of the tunnel

Ding et al. adopted the numerical analysis method to simulate the air flow distribution in three hearts arch-section tunnels and testified on the accuracy of the numerical analysis method. In this paper, the tunnel length is 8 m, the width is 260 mm, and wall height is 113 mm. The small arch radius is 66 mm, and the large arch radius is 183 mm, as shown in Figure 1.

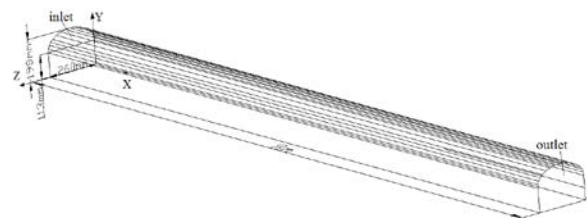


Figure 1: The physical model of the tunnel.

In order to analyze the air flow structure in tunnels quantitatively, the model in Figure 1 was amplified by 2 times, 3 times, 4 times, and 5 times. The sizes of the five three hearts arch-section tunnels are shown in Table 1. The air flow in the tunnels was set to be turbulent, which was similar to the actual ventilation conditions. The air flow distribution was

*Corresponding author--email:cui_ding@163.com

Table 1: The sizes of the five three hearts arch tunnels .

Tunnel number	Tunnel parameters				
	large archradius(mm)	Smaller chradius(mm)	width(mm)	Wall height(mm)	length(m)
1	183	66	260	113	8
2	366	132	520	226	16
3	549	198	780	339	24
4	732	264	1040	452	32
5	915	330	1300	565	40

then studied under different air flow velocities and different tunnel sizes.

2.2 Mathematical model and assumptions

According to the fluid dynamics theory, the air flow in tunnels can be described by using the following equations.

The continuity equation:

$$\frac{\partial \rho}{\partial t} + \frac{\partial(\rho u_j)}{\partial x_j} = 0$$

The momentum equations(i direction):

$$\frac{\partial(\rho u_i)}{\partial t} + \frac{\partial(u_j u_i)}{\partial x_j} = \frac{\partial}{\partial x_j} \left(\mu \frac{\partial u_j}{\partial x_j} \right)$$

The energy equation:

$$\frac{\partial(\rho h)}{\partial t} - \frac{\partial(\rho u_j h)}{\partial x_j} = \frac{\partial}{\partial x_j} \left(\Gamma_h \frac{\partial h}{\partial x_j} \right)$$

The standard k-ε model was used to calculate the turbulence and diffusion of the air flow.

k equation:

$$\begin{aligned} \frac{\partial}{\partial t}(\rho k) + \frac{\partial}{\partial x_i}(\rho k u_i) \\ = \frac{\partial}{\partial x_j} \left[\left(\mu + \frac{\mu_t}{\sigma_k} \right) \frac{\partial k}{\partial x_j} \right] + G_k - \rho \epsilon \\ - Y_M \end{aligned}$$

ε equation:

$$\begin{aligned} \frac{\partial}{\partial t}(\rho \epsilon) + \frac{\partial}{\partial x_i}(\rho \epsilon u_i) \\ = \frac{\partial}{\partial x_j} \left[\left(\mu + \frac{\mu_t}{\sigma_\epsilon} \right) \frac{\partial \epsilon}{\partial x_j} \right] + C_{1\epsilon} \frac{\epsilon}{k} G_k \\ - C_{2\epsilon} \rho \frac{\epsilon^2}{k} \end{aligned}$$

In these equations, G_k represents the generation of turbulence kinetic energy due to the mean velocity gradients, $G_k = -\rho u_i \overline{u_j} \frac{\partial u_j}{\partial x_i}$. Y_M represents the contribution of the fluctuating dilatation in compressible turbulence to the overall dissipation

rate, $Y_M = 2\rho \epsilon M_t^2$. μ_t represents the turbulent viscosity, $\mu_t = \rho C_\mu \frac{k^2}{\epsilon}$.

$C_{1\epsilon}$, $C_{2\epsilon}$ and C_μ are constants. $C_{1\epsilon} = 1.44$, $C_{2\epsilon} = 1.92$, $C_\mu = 0.09$. σ_k and σ_ϵ are the turbulent Prandtl numbers for k and ε, respectively. $\sigma_k = 1.0$, $\sigma_\epsilon = 1.3$.

ρ represents the density, kg/m³. u represents the velocity, m/s. k represents the turbulence kinetic energy, kJ/kg. ϵ represents the turbulence kinetic energy dissipation rate, m²/s³. μ represents the molecular (dynamic) viscosity, Pa.s. t represents the time, s. h represents the static enthalpy, k. Γ_h represents the transport coefficient.

When developing the mathematical model, the following assumptions were made: the air flow was incompressible; the wall was adiabatic; there were no workers and vehicles in the tunnels, and the presence of smoke and dust were ignored.

2.3 Boundary Conditions and Parameters

The tunnel inlet was set to be the velocity-inlet and the air flow velocity was set to 1m/s, 2m/s, 3m/s, 4m/s and 5m/s respectively. The tunnel outlet was set to be the pressure-outlet and the relative pressure was 0 Pa. The air flow distribution in the three hearts arch-section tunnels of five sizes were simulated under the different air flow velocities.

3. ANALYSIS OF THE AIR FLOW STRUCTURE IN TUNNELS

The air flow distribution on fully developed turbulence cross sections were studied. In this paper, the distance between the cross sections analyzed and the tunnel inlet was set according to fluid mechanics theory, and the distance between the analyzed cross sections and the tunnel inlet was 5.6 m (Z_1), 11.2 m (Z_2), 16.8 m (Z_3), 22.4 m (Z_4), 28 m (Z_5),

respectively. The velocity profiles on the above five cross sections (Z_1, Z_2, Z_3, Z_4, Z_5) were analyzed as shown in Figure 2.

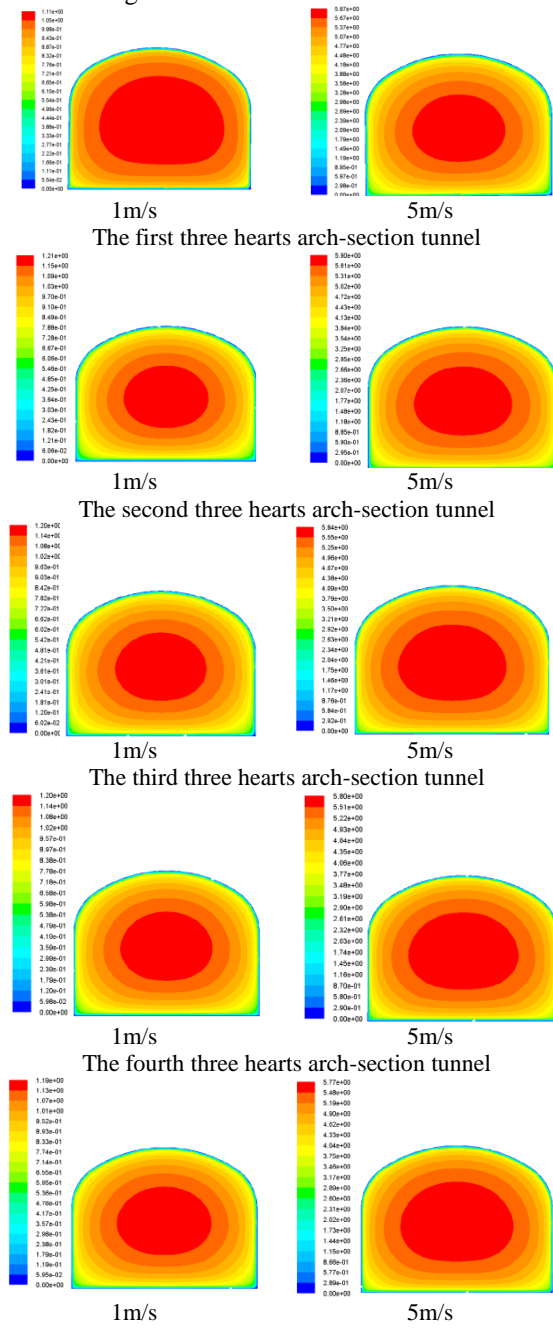


Figure 2: Velocity profiles on fully developed turbulence sections in five tunnels.

It can be concluded from Figure 2 that the air flow structure showed a circular distribution which was similar to the shape of three hearts arch-section under different ventilation velocities and cross section sizes. The shape of the cross section was the critical factor influencing the air flow structure. The

air flow velocity reached its maximum value in the center of the tunnel and decreased from the center to the tunnel wall. The average velocity points were mainly close to the tunnel wall under different air flow velocities and the air flow velocity which was smaller than the average velocity would decrease more quickly when it was closer to the tunnel wall. According to the above analysis, the tunnel wall was also a critical factor influencing the air flow distribution.

4. ANALYSIS OF AVERAGE VELOCITY DISTRIBUTION

The average velocity points are critical to achieving an accurate measurement and monitoring of ventilation volumes in tunnels. According to Ding (Ding et al., 2015), the distribution of the average velocity points in any three hearts arch-section tunnel shows as an annular ring and the ventilation velocity has little influence on the above distribution feature. In order to further analyze the distribution of the average velocity points and develop its characteristic equations, the distribution curve has been separated into six parts as shown in Figure 3.

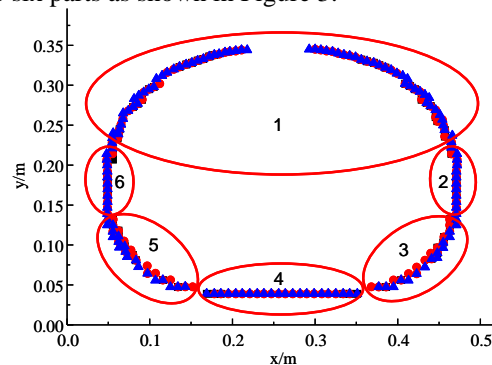


Figure 3: The average distribution curve on three hearts arch-section.

According to Ding (Ding et al., 2015), the characteristic equation of the first part can be described by equation 1-1, and in this paper, the characteristic equations of the other five parts are developed.

$$3.2819r_1^{-2} \left(x - \frac{d}{2} \right)^2 + 8.408r_1^{-1.84} (y - 0.6142r_1 + 0.0138)^2 = 1 \quad (1-1)$$

r_1 — radius of the top circular arc, m ;

d — width of the tunnel, m.

As shown in Figure 3, the curve is symmetrical, so the feature of the fourth, fifth, and sixth parts will be analyzed quantitatively.

(1) The fourth part

Based on an analysis of relationships between the length of the fourth part curve, the tunnel size and the distance between the curve and the tunnel floor, it

has been found that the length of the fourth part curve and the distance between the curve and the tunnel floor had perfect linear relations with the width of the tunnel as shown in Figures 4 and 5, respectively.

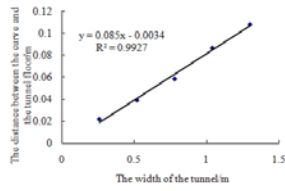


Figure 4: Relationship between the distance from the bottom edge to part 4 and the length of bottom edge.

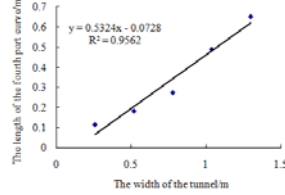


Figure 5: Relationship between the length of part 4 and the length of the bottom edge.

Based on the above analysis, the characteristic equations of the fourth part can be described as equations 1-2 and 1-3.

$$d_1 = 0.085d - 0.0034 \quad (1-2)$$

$$d_2 = 0.5324d - 0.0728 \quad (1-3)$$

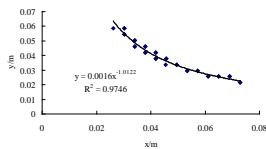
d —width of the tunnel, m ;

d_1 — distance between the fourth part curve and the tunnel floor, m ;

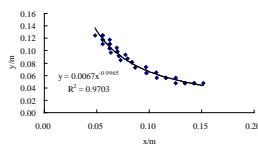
d_2 —length of the fourth part curve, m.

(2) The fifth part

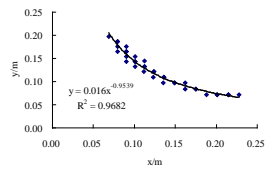
Numerical fitting methods have been used to develop the characteristic equations of the fifth part as shown in Figure 6.



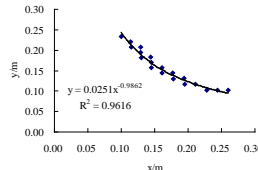
The first three hearts arch-section tunnel



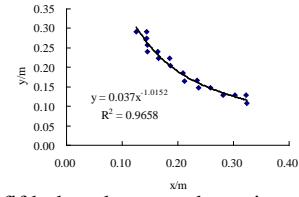
The second three hearts arch-section tunnel



The third three hearts arch-section tunnel



The fourth three hearts arch-section tunnel



The fifth three hearts arch-section tunnel

Figure 6: Part 5 curve fitting diagram of three hearts arch-sections in five tunnels.

By combining the above five equations and the width of different tunnels, the five equations can be normalized into one equation, equation 1-4.

$$y = 0.0236d^{1.965}x^{-1} \quad (1-4)$$

d —width of the tunnel, m ;

x —x-coordinate, $m, x \in [0.2219h - 0.0014, 0.2338d + 0.0364]$

y — y-coordinate, m.

(3) The sixth part

The feature of the sixth part has been studied using the above method. The length of the curve and the distance between the curve and the left wall have a perfect linear relation with the height of the tunnel wall, as shown in Figures 7 and 8.

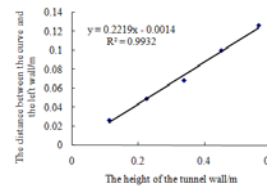


Figure 7: Relationship between the distance from part 6 to the left edge and the height of the wall.

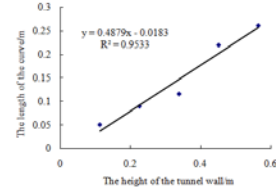


Figure 8: Relationship between the length of part 6 and the height of the wall.

Based on the above analysis, the characteristic equations of the sixth part can be represented by equations 1-5 and 1-6.

$$h_1 = 0.2219h - 0.0014 \quad (1-5)$$

$$h_2 = 0.4879h - 0.0183 \quad (1-6)$$

h —height of the tunnel wall, m;

h_1 —distance between the sixth part curve and the left wall, m;

h_2 —length of the curve, m.

Based on the above analysis, the characteristic equations of all the six parts have been developed as shown in Table 2.

Table 2: Characteristic equations of three hearts arch-section tunnel.

Serial number	Characteristic equations	span of the parameters
1	$3.2819r_1^{-2}\left(x - \frac{d}{2}\right)^2 + 8.408r_1^{-1.84}(y - 0.6142r_1 + 0.0138)^2 = 1$	$y \geq 0.9932h - 0.0087$
2	$x = d - 0.2219h + 0.0014$	$y \in [0.5053h + 0.0096, 0.9932h - 0.0087]$
3	$f(x) = 0.0236d^{1.965}(d - x)^{-1}$	$x \in (0.7662d - 0.0364, d - 0.2219h + 0.0014)$
4	$f(x) = 0.085d - 0.0034$	$x \in [0.2338d + 0.0364, 0.7662d - 0.0364]$
5	$f(x) = 0.0236d^{1.965}x^{-1}$	$x \in (0.2219h - 0.0014, 0.2338d + 0.0364)$
6	$x = 0.2219h - 0.0014$	$y \in [0.5053h + 0.0096, 0.9932h - 0.0087]$

5. CONCLUSIONS

In order to understand the air flow distribution in tunnels and measure the average velocity and ventilation volume accurately, the air flow structure and the average velocity points in different sizes of three hearts arch-section tunnels were investigated. The conclusions were as follows:

1) The air flow structure showed a circular distribution which was similar to the shape of three hearts arch-section under different ventilation velocities and cross section sizes. The shape of the cross section was the critical factor influencing the air flow distribution. The air flow velocity reached its maximum value in the center of the tunnel and decreased from the center to the tunnel wall.

2) The average velocity points were mainly close to the tunnel wall under different air flow velocities and the air flow velocity which was smaller than the average velocity would decrease more quickly when it was closer to the tunnel wall. The tunnel wall was also a critical factor influencing the air flow distribution.

3) Characteristic equations were developed to describe the average velocity distribution, which provide the theoretical basis for accurately measuring the average velocity and ventilation volume in mine tunnels.

6. ACKNOWLEDGEMENT

This research has been funded by the central university basic business expenses(15zy012)

7. REFERENCES

Chen W, Yu X. (2008) Wind flow field simulation on wind pink piping basing on FLUENT. Jiangsu Electrical Engineering, Volume 27, No.6, pp.72-75.

Ding C, He X, Nie B. (2015) Numerical and experimental research on "key ring" distribution of ventilation in mine tunnels. Journal of Liaoning Technical University (Natural Science), Volume34, No. 10, pp.1131-1136

Ding C. (2016) Numerical and experimental research on the average velocity distribution in the trapezoid tunnels. Journal of Safety Science and Technology, Volume12, No. 1.

Hao Y, Chen K, Jiang Z et al. (2011) Study on Amendment of Airflow Velocity in Roadway Based on CFD. Safety in Coal Mines, Volume42, No. 2, pp. 1-4.

Jia J. (2011) Simulation analysis on mine wind monitoring. Coal, Volume 20, No.12, pp. 73-74.

MA Y, Dong B, Zhang X et al. (2007) Study on Vent Mean Wind Velocity Measuring of Solar Collecting Wall in Solar House. Building Energy & Environment, Volume26, No. 4, pp. 60-63.

M.T. Parra, J.M. Villafuella, F. Castro, C. Me'ndez. (2006) Numerical and experimental analysis of different ventilation systems in deep mines. Building and Environment, Volume 41, pp. 87-93.

Tan X, Wang Z, Zhao Y. et al. (2013) Study on Velocity Profile of Turbulent Fluid in Narrow Deep Type Rectangular Channel. Journal of Sichuan University (Engineering Science Edition), Volume45, No. 6, pp.67-73.

Wang B, Luo Y, Zhao Y. (2013) Wind Tunnel Simulation on Wind Speed Distribution Characteristic in Rectangle Roadway Section Laid With Conveyor. Safety in Coal Mines, Volume44, No. 5, pp. 42-45.

Yin J, Lv H, Luan W. et al. (2008) Experimental research on velocity distribution law of trapezoidal channel section. Yangtze River, Volume39, No. 12, pp. 67-69.

Zhao D, Huang F, Chen S. et al. (2014) Relationship between point air velocity and average air velocity in circular roadway. Journal of Liaoning Technical University (Natural Science), Volume33, No. 12, pp.1654-1659.

Zhou X, Meng L, LI C. et al. (2012) Experimental study on determination and correction method of wind speed in circular pipe. Journal of Liaoning Technical University: Natural Science, Volume31, No. 6, pp. 801-804.